dLKR/SDH regulates hormone-mediated histone arginine methylation and transcription of cell death genes

Dimitrios Cakouros, Kathryn Mills, Donna Denton, Alicia Paterson, Tasman Daish, and Sharad Kumar

Hanson Institute, Institute of Medical and Veterinary Science, Adelaide SA 5000, Australia

The sequential modifications of histones form the basis of the histone code that translates into either gene activation or repression. Nuclear receptors recruit a cohort of histone-modifying enzymes in response to ligand binding and regulate proliferation, differentiation, and cell death. In *Drosophila melanogaster*, the steroid hormone ecdysone binds its heterodimeric receptor ecdysone receptor/ultraspiracle to spatiotemporally regulate the transcription of several genes. In this study, we identify a novel cofactor, *Drosophila* lysine ketoglutarate reductase (dLKR)/saccharopine dehydrogenase (SDH), that is involved in ecdysone-mediated transcription. dLKR/SDH binds histones H3 and H4 and suppresses ecdysone-mediated transcription of cell death genes by inhibiting histone H3R17me2 mediated by the *Drosophila* arginine methyl transferase CARMER. Our data suggest that the dynamic recruitment of dLKR/SDH to ecdysone-regulated gene promoters controls the timing of hormone-induced gene expression. In the absence of dLKR/SDH, histone methylation occurs prematurely, resulting in enhanced gene activation. Consistent with these observations, the loss of dLKR/SDH in *Drosophila* enhances hormone-regulated gene expression, affecting the developmental timing of gene activation.

Introduction

The N-terminal tails of histones are subject to diverse post-translational modifications such as acetylation, methylation, phosphorylation, ubiquitination, and sumoylation (Kouzarides, 2007; Li et al., 2007). Distinct modifications act sequentially or in combination to form the histone code (Strahl and Allis, 2000). These modifications provide a platform recognition surface for nonhistone proteins that translate the histone code to ultimately affect many biological processes, including gene expression, DNA replication, and repair (Kouzarides, 2007; Li et al., 2007).

Although histone acetylation/deacetylation has been studied extensively, dynamics of histone methylation was the subject of considerable debate, as it was long thought to be a stable epigenetic modification because of the absence of a known histone demethylase. Chromatin immunoprecipitation (ChIP)

studies have revealed that histone methylation on both lysine and arginine residues can be extremely dynamic on various promoters and in response to specific signals (Bannister et al., 2002; Metivier et al., 2003). Methylation of arginine residues on histone 3 (H3) by CARM1 and histone 4 (H4) by PRMT1 is known to occur in response to nuclear hormones (Chen et al., 1999; Wang et al., 2001). The discovery of PADI4 lent support to the dynamic nature of histone methylation, as it was demonstrated to deiminate both the unmodified and monomethylated forms of histone H3R2, R17, and R26, forming citrulline and thereby antagonizing histone arginine methylation (Cuthbert et al., 2004). This was followed by identification of the first lysine-specific demethylase, LSD1, a nuclear amine oxidase that was found to demethylate H3K4me1 and me2 in a flavin adenine dinucleotide–dependent oxidative reaction (Shi et al., 2004). This is consistent with the finding that LSD1 is part of the Co-REST repressor complex (Ballas et al., 2001). The discovery of JHDM1A (FBXL11), which specifically demethylates histone

Correspondence to Sharad Kumar: sharad.kumar@imvs.sa.gov.au

Abbreviations used in this paper: ARK, Apaf1-related killer; BE, binding element; BR-C, broad complex; ChIP, chromatin immunoprecipitation; dLKR, *Drosophila* LKR; EcR/Usp, ecdysone receptor/ultraspiracle; EMSA, electrophoretic mobility shift assay; LKR, lysine ketoglutarate reductase; SDH, saccharopine dehydrogenase; TRR, trithorax-related protein.

The online version of this article contains supplemental material.

The Rockefeller University Press $30.00
J. Cell Biol. Vol. 182 No. 3   481–495
www.jcb.org/cgi/doi/10.1083/jcb.200712169

JCB   481

H3K36 using Fe (II) and α-ketoglutarate as cofactors (Tsukada et al., 2006), led to the establishment of the third family of demethylases, the JmjC domain–containing histone demethylases. This family is evolutionarily conserved with 30 proteins in humans and mice and 13 in *Drosophila melanogaster* (Klose et al., 2006; Shi and Whetsine, 2007). It is now apparent that the dynamics of histone methylation is a tightly regulated process involving both histone methyltransferases and histone-specific demethylases. As more demethylases will inevitably be discovered, the question arises as to how the rapid kinetics of histone arginine methylation/demethylation is controlled at the molecular level and how this relates to the dynamics of other histone modifications involved in the histone code in response to a given signal.

Nuclear receptors are ligand-activated transcription factors that bind to target gene promoters. In the presence of ligand, they recruit coactivators to modify and remodel the chromatin structure, which ultimately leads to the assembly of the RNA polymerase II–containing transcription complex (Tsai and Fondell, 2004). A ligand-induced conformational change results in direct recruitment of the p160 coactivators, further recruiting p300/CREB-binding protein (CBP) and coactivator-associated arginine methyltransferase (CARM1), which methylates histones H3R2, R17, and R26 (Chen et al., 1999; Schurter et al., 2001). In *Drosophila*, the major metamorphic transitions during development are mediated by the steroid hormone ecdysone, which binds its heterodimeric receptor, ecdysone receptor/ultraspiracle (EcR/Usp), and regulates proliferation, programmed cell death, and differentiation in a tissue- and developmental-specific manner (Lee et al., 2002; for reviews see Truman and Riddiford., 2002; Kumar and Cakouros, 2004; Yin and Thummel, 2005). An ecdysone pulse toward the end of the larval stage signals puparium formation and histolysis of the larval midgut. A second ecdysone pulse ∼12 h later initiates head eversion and histolysis of the larval salivary glands (Lee et al., 2002; for reviews see Truman and Riddiford, 2002; Kumar and Cakouros, 2004; Yin and Thummel, 2005). Previously, we discovered that the caspase *dronc* is dramatically up-regulated in dying larval salivary glands in response to ecdysone (Dorstyn et al., 1999; Cakouros et al., 2002), and this is partly the result of direct binding of EcR/Usp to the promoter that controls its temporal expression (Daish et al., 2003; Cakouros et al., 2004a). DRONC and its adaptor Apaf1-related killer (ARK) are essential for ecdysone-mediated cell death of larval salivary glands (Daish et al., 2004; Akdemir et al., 2006; Mills et al., 2006). We also found that the arginine histone methyltransferase CARMER/DART4 is associated with EcR/Usp (Cakouros et al., 2004b).

In this study, we identify a novel cofactor, *Drosophila* lysine ketoglutarate reductase (LKR [dLKR])/saccharopine dehydrogenase (SDH), that binds EcR/Usp and regulates hormone-mediated transcription. dLKR/SDH specifically inhibits CARMER-mediated H3R17me2 by directly interacting with histone H3 but does not inhibit H3K4me3, which is also induced by ecdysone. dLKR/SDH genetically interacts with EcR/Usp and is recruited to hormone-responsive promoters to control the kinetics of H3R17me2.

Results

dLKR/SDH is recruited to the EcR/Usp-binding element

In *Drosophila*, the only known coactivators for EcR/Usp are Taiman (p160 coactivator), CARMER, and the trithorax-related protein (TRR; a histone lysine methyltransferase). To identify other factors, we used the immobilized template bead assay in which the EcR/Usp-binding element (BE) of the caspase *dronc* promoter was biotin tagged, immobilized onto streptavidin beads, and incubated with nuclear extracts from *Drosophila l*(2)mbn cells with or without ecdysone treatment. *l*(2)mbn cells have been used in the past for characterizing ecdysone-mediated transcription and apoptosis (Cakouros et al., 2002, 2004b). To verify recruitment of the EcR-B1 isoform to the *dronc* promoter, the bound extracts were subjected to immunoblotting, which demonstrated the recruitment of EcR-B1 to the template in both the absence and presence of ecdysone treatment (Fig. 1 A, bottom). However, recruitment to the mutated EcR/Usp BE template was reduced as expected. This mutation, which alters the consensus binding site for EcR/Usp, has been previously described (Cakouros et al., 2004a). Several proteins were identified by mass spectrometry to be specifically recruited to the wild-type EcR/Usp BE in the presence of ecdysone. These included CG10473, which is involved in chromatin condensation; CG10223 (topoisomerase II), which is involved in transcription from polymerase II promoters; a zinc finger protein, CG10084; an unknown methyltransferase, CG8545; a helicase, CG6375; as well as an uncharacterized protein (CG7144) of ∼110 kD that we have called dLKR/SDH (Fig. 1 A, top).

dLKR/SDH is an evolutionarily conserved protein with homologues in *Arabidopsis thaliana* (SDH or LKR/SDH), yeast (Lys9 and Lys1), *Drosophila*, mouse, and human (aminoadipate semialdehyde synthase). It is a dual activity enzyme with an N-terminal LKR domain and a C-terminal SDH domain (Sacksteder et al., 2000). Except in *Saccharomyces cerevisiae*, in which *Lys1* encodes for the LKR and *Lys9* encodes for the SDH enzyme, bifunctional LKR/SDH is encoded by a single protein. dLKR/SDH is 51% identical and 71% similar to mouse and human LKR/SDH. In *A. thaliana*, yeast, mice, and humans, this enzyme is involved in catabolism of lysine to saccharopine by the LKR domain (Fig. 1 B) and from saccharopine to amino adipate semialdehyde by the SDH domain (Bhattacharjee, 1985; Goncalves-Butruille et al., 1996; Sacksteder et al., 2000; Zhu et al., 2000). The reaction uses NADH and α-ketoglutarate in the first step, which is oxidized to NAD^+, and then NAD^+ is used for the conversion to amino adipate semialdehyde. In yeast, these reactions are reversible and can produce lysine from saccharopine; however, mammalian LKR/SDH is unable to do this (Sacksteder et al., 2000).

Using GST fusion proteins of both individual enzyme domains (LKR and SDH) and in vitro–translated EcR-B1, the direct association of the carboxyl SDH domain with the EcR-B1 isoform was observed both in the absence and presence of ecdysone, whereas the LKR domain displayed a much weaker interaction in both the absence and presence of ecdysone (Fig. 1 C). To further narrow the binding region, we sequentially deleted
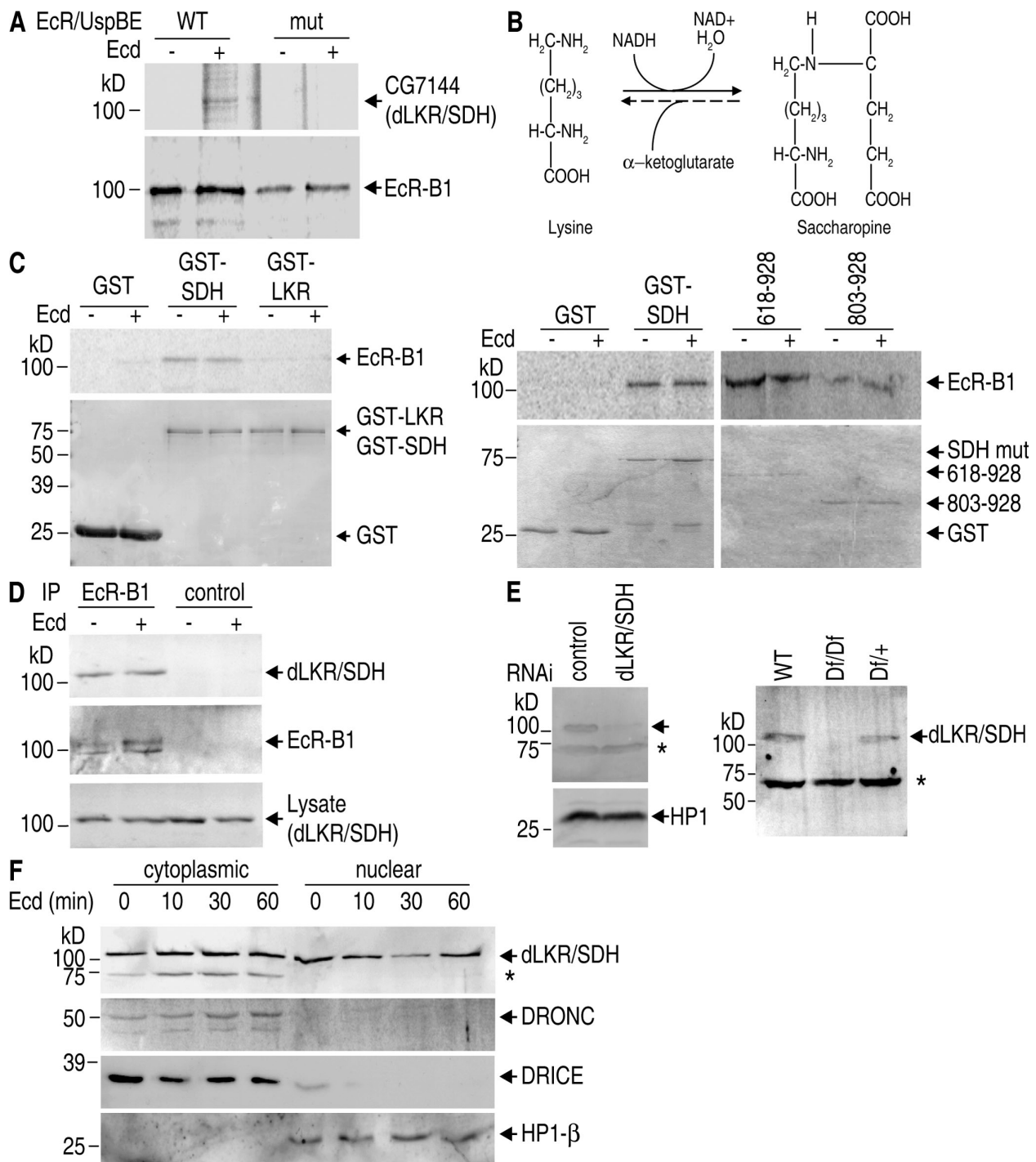
Figure 1. **dLKR/SDH is recruited to the _dronc_ promoter and localizes to the cytoplasm and nucleus.** (A) Nuclear extracts from cells treated with either ethanol (−) or 10 µM ecdysone (Ecd +) for 2 h were incubated with double-stranded biotin-tagged wild-type (WT) or mutated (mut) oligonucleotides corresponding to the _dronc_ EcR/Usp BE and pulled down with streptavidin beads. Proteins were separated by SDS-PAGE and stained, and protein bands were isolated. Part of the pull-down was blotted with EcR-B1 antibody. (B) LKR converts lysine to saccharopine by oxidizing NADH to NAD^+ and condensing α-ketoglutarate molecule onto the amino group. (C) GST, GST-LKR, GST-SDH, and GST-SDH deletion mutants containing the indicated residues (618–928 or 803–928) were used in pull-down experiments with ^{35}S-labeled EcR/Usp in the presence of ethanol control (−) or ecdysone (+). Half of the reaction was used in SDS-PAGE and stained with Coomassie Brilliant blue. (D) Lysates from cells treated with ethanol (−) or ecdysone (Ecd +) for 4 h were immunoprecipitated (IP) with EcR-B1 or a control (N27A1) antibody and blotted with dLKR/SDH and EcR-B1 antibodies. The bottom panel is a dLKR/SDH immunoblot of the lysates used in immunoprecipitation. (E) 200 ng/ml of affinity-purified dLKR/SDH antibody was used to blot extracts from _l_(2)mbn cells treated with a control (Ndfip2) dsRNA or dLKR/SDH dsRNA. Lysates from either wild-type, homozygous (_Df/Df_), or heterozygous (_Df/+_) _Drosophila_ carrying a deficiency that removes the dLKR/SDH locus were probed with the dLKR/SDH antibody. This antibody cross reacts with a nonspecific protein (asterisks) of ∼65 kD (here and elsewhere in immunoblots). dLKR/SDH protein bands are indicated by arrows. The same filter was blotted with heterochromatin protein 1 (HP1). (F) _l_(2)mbn cells were treated with ethanol (0) or ecdysone as indicated, and nuclear and cytoplasmic fractions were blotted with the indicated antibodies.

the SDH domain. Although the region spanning amino acids 618–928 bound EcR/Usp efficiently, further deletion to residue 803 diminished binding (Fig. 1 C). Endogenous EcR-B1 immunoprecipitated with dLKR/SDH both in the absence and presence of ecdysone (Fig. 1 D). An antibody raised in rabbits identified a 110-kD dLKR/SDH protein in l(2)mbn cells and *Drosophila* larvae. This protein is nearly ablated by dLKR/SDH RNAi in l(2)mbn cells, absent in a homozygous dLKR/SDH genetic deficiency, and reduced in heterozygous animals (Fig. 1 E).

To determine the subcellular localization of dLKR/SDH, fractionation experiments were performed using lysates from l(2)mbn cells. dLKR/SDH was readily detectable in the cytosol of both untreated and ecdysone-treated cells. dLKR/SDH was also seen in nuclear extracts, and the protein levels appeared to be dynamic upon ecdysone treatment, decreasing at 10–30 min of treatment and increasing by 1 h (Fig. 1 F). The same membrane was blotted for cytosolic proteins DRONC and DRICE as well as the nuclear heterochromatin protein 1 (HP1-β), demonstrating the purity of the fractions. Our antibody was unsuitable for immunohistochemical detection of the low levels of endogenous dLKR/SDH protein (unpublished data). Therefore, we further analyzed dLKR/SDH localization by expressing a tagged version of the protein in l(2)mbn cells. As shown in Fig. S1 (available at http://www.jcb.org/cgi/content/full/jcb.200712169/DC1), ectopically expressed dLKR/SDH localized to both the cytosol and nucleus.

dLKR/SDH represses ecdysone-mediated transcription

To test the effect of dLKR/SDH on ecdysone-mediated transcription, we expressed and purified full-length His-tagged dLKR/SDH from insect cells. By using lysine as a substrate, we measured oxidation of NADH to NAD^+ and observed a time-dependent decrease in NADH, implying that the full-length protein is enzymatically active (Fig. 2 A). l(2)mbn cells were therefore transfected with a promoter-reporter (pEcR-Luc) that is activated by direct binding of the preexisting EcR/Usp complex. This reporter was activated by ecdysone and repressed by coexpressing increasing amounts of dLKR/SDH, indicating a direct effect on the EcR/Usp complex (Fig. 2 B). Given the high conservation of dLKR/SDH throughout evolution, the putative NADH-binding domain, which is responsible for enzymatic activity, was identified based on homology to the extensively characterized yeast homologue. This domain was mutated (see Oligonucleotides and primers section), and its effect on reporter expression was examined. The mutated dLKR/SDH was enzymatically inactive (unpublished data). As shown in Fig. 2 C, there was no significant difference in the repressive ability of the mutant and wild-type proteins, suggesting that the repressive effect is independent of dLKR/SDH's catalytic activity. In contrast, overexpression of dLKR/SDH had no significant repressive effect on transcription mediated by an unrelated transcription factor, broad complex (BR-C), when driving expression of a BR-C–regulated promoter-reporter (Fig. 2 D). In support of its role as a repressor of ecdysone-mediated transcription, knockdown of dLKR/SDH resulted in a significant increase in ecdysone-induced reporter activity (Fig. 2 E), whereas no effect was evident on the BR-C reporter (Fig. 2 F).
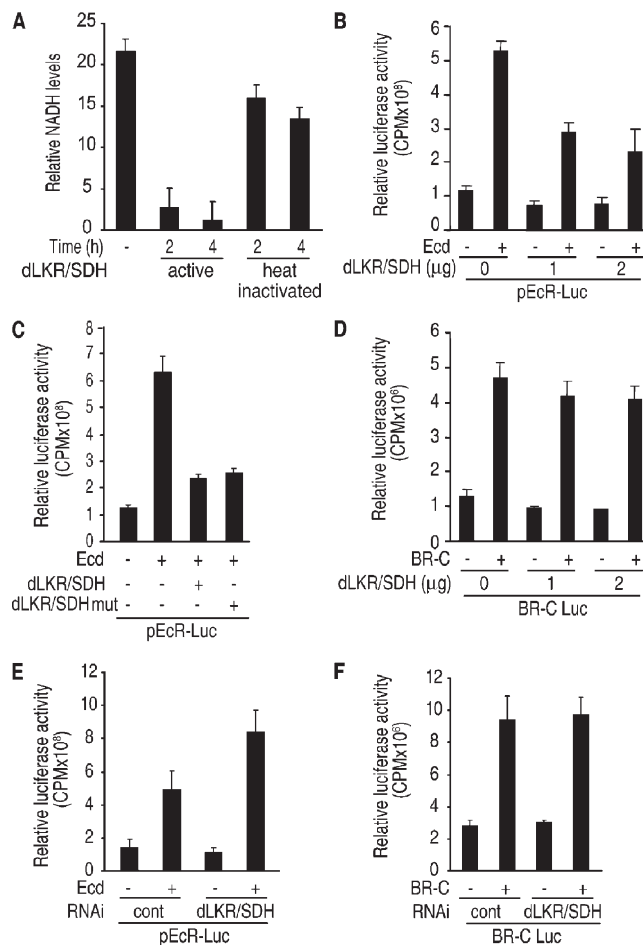

Figure 2. **dLKR/SDH represses ecdysone receptor–mediated transcription.** (A) 5 μg of recombinant active or heat-inactivated dLKR/SDH was incubated with 1 mM NADH, 2 mM α-ketoglutarate, and 14 mM lysine. Buffer without enzyme (−) was incubated for 4 h before measuring NADH levels. Two experiments were performed in triplicate. (B) 2.5×10^6 cells were transfected with 1 μg luciferase reporter driven by the EcR BE of the Hsp 27 promoter (pEcR-Luc) and pIB dLKR/SDH (dLKR/SDH) in the presence of ethanol (−) or 10 μM ecdysone (Ecd +). Each experiment was performed in triplicate, and total DNA was made up to equal amounts using vector. 30 μg of lysate was assayed for luciferase activity. Data were derived from at least three experiments. (C) Same as in B, but the NADH domain of dLKR/SDH was mutated by substituting amino acids 221, 223, and 228 to alanine (dLKR/SDH mut). (D) Experiments performed as in B, but a luciferase reporter with the proximal promoter of *dronc* containing multiple BR-C BEs was used (BR-C Luc). Either empty expression vector pIE (−) or vector expressing BR-C (+) was cotransfected where indicated. (E) Experiments performed as in B, but dsRNA corresponding to mammalian Ndfip2 (cont) or dLKR/SDH was included with pEcR-Luc. Ethanol vehicle (−) or ecdysone (+) was included as shown. (F) Experiments performed as in D using the BR-C reporter (BR-C Luc) and the transcription factor BR-C overexpressed where indicated (+). dsRNA (RNAi) corresponding to Ndfip2 (cont) or dLKR/SDH was included where indicated. Error bars represent SD.

To further study the function of dLKR/SDH on hormone-induced transcription, ecdysone-induced transcription of the cell death genes *ark* and *dronc* was assessed after knockdown of dLKR/SDH in l(2)mbn cells. As assessed by semiquantitative real-time PCR, dLKR/SDH expression was reduced by 80% (Fig. S2, available at http://www.jcb.org/cgi/content/full/jcb.200712169/DC1). Both *ark* and *dronc* transcription increased after ecdysone treatment (Fig. 3 A). When dLKR/SDH was knocked down, transcription of both *dronc* and *ark* was significantly
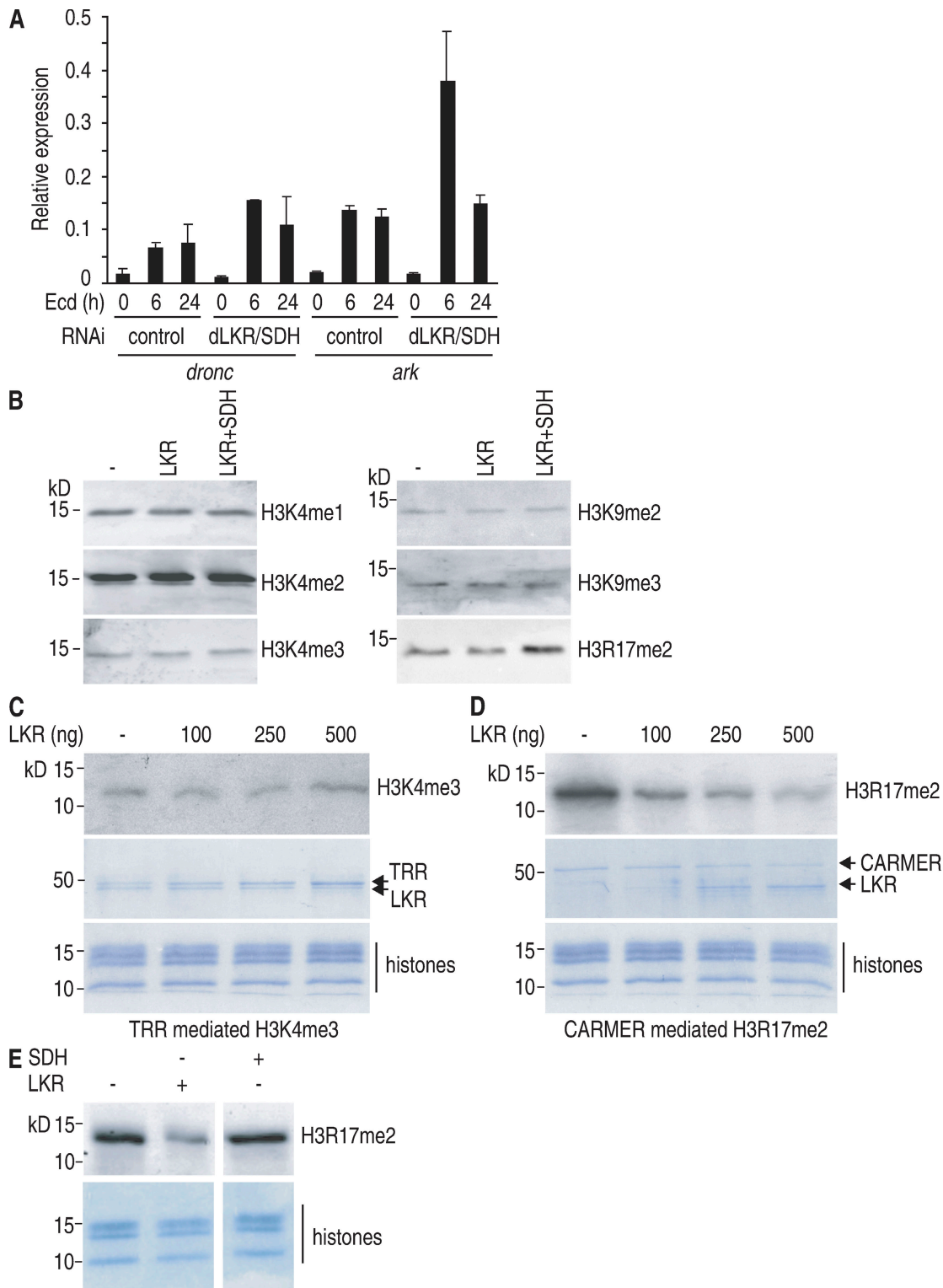
Figure 3. **Knockdown of dLKR/SDH potentiates *dronc* and *ark* transcription, and dLKR/SDH inhibits H3R17 methylation in vitro.** (A) *l*(2)mbn cells were treated with dsRNA (RNAi) corresponding to mammalian Ndfip2 (control) or with dLKR/SDH and ethanol (0) or ecdysone (Ecd) for 6 or 24 h in triplicate. Levels of *dronc* and *ark* transcript were measured using real-time PCR and expressed relative to the internal housekeeping gene ribosomal protein *rp49*. Error bars represent SD. (B) 4 μg of calf thymus histones were incubated alone (−) or with 500 μg of recombinant GST-LKR (LKR) or GST-SDH (SDH) protein individually or together (LKR + SDH) for 4 h in the presence of NADH and α-ketoglutarate and were blotted with histone methylation–specific antibodies recognizing H3K4me1, H3K4me2, H3K4me3, H3K9me2, H3K9me3, and H3R17me2. H3R17me2 was assessed by methylating calf thymus histones first with CARMER before incubation with GST LKR/SDH. (C and D) 4 μg of calf thymus histones were incubated with increasing amounts of recombinant LKR (thrombin cleaved to remove GST) for 4 h. To the same reaction, 1 μg of either TRR or CARMER was added in methylation buffer (including ^{3}H S-adenosyl methionine) for 90 min. Half of the total reaction was separated by SDS-PAGE and Coomassie stained, whereas the other half was electrophoresed, fixed, incubated in Amplify, dried, and exposed to hyperfilm. Methylation by TRR (H3K4me3) and CARMER (H3R17me2) are shown, as are total histones, dLKR/SDH, GST-TRR, and GST-CARMER. (E) Reactions performed as in C and D, including the addition of the SDH domain. Methylation by CARMER (H3R17me2) is shown, and Coomassie staining of histones in each sample is shown on the bottom panel.

increased in response to ecdysone treatment, with the greatest effect evident at 6 h of ecdysone treatment. Overall, the results suggest that dLKR/SDH negatively regulates hormone-induced transcription, and knocking down its expression alters the transcription kinetics of ecdysone-induced cell death genes.

Methylation of H3R17 is inhibited by dLKR/SDH

Given that the histone demethylase PADI4 demethylates histone H3 on arginine 17 (R17) and also plays a role in amino acid catabolism, we postulated that dLKR/SDH might be involved in demethylating histones. This was examined using calf thymus histones, recombinant LKR or SDH domain, and appropriate cofactors. The LKR domain alone or together with the SDH domain did not demethylate H3K4me1, me2, me3, H3K9me2, me3, or H3R17me2 (H3R17me1 could not be detected; Fig. 3 B). The same results were obtained when using purified histones from HeLa cells (unpublished data). We next examined whether dLKR/SDH might inhibit histone methylation mediated by histone methyltransferases involved in hormone-mediated transcription. To test this, histones were incubated with increasing amounts of the LKR domain and were methylated with either TRR, which mediates H3K4me3, or CARMER, which mediates H3R17me2. The LKR domain had no significant effect on H3K4me3 but strongly inhibited H3R17me2 in a dose-dependent manner (Fig. 3, C and D). However, the SDH domain had no significant effect on the methylation of histone H3 (Fig. 3 E).

To determine whether dLKR/SDH modifies histones and therefore inhibits methylation, we incubated full-length purified dLKR/SDH with histone H3, NADH, and α-ketoglutarate. We did not detect any specific histone H3 modifications mediated by dLKR/SDH as determined by mass spectrometry, suggesting that dLKR/SDH-mediated inhibition of H3R17me2 is not driven by its enzymatic activity (unpublished data).

dLKR/SDH directly interacts with H3 and H4 and inhibits CARMER-mediated transcription

We next examined the direct interaction of the LKR domain with purified histones. GST-LKR specifically associated with histone H3 as shown by H3-specific antibodies (Fig. 4 A). Furthermore, protein staining showed that the LKR domain interacted specifically with H3 and H4 but not H2B or H2A (Fig. 4 A). The region of histone H3 that interacts with the LKR domain was determined by competition experiments using histone H3 peptides. Peptides corresponding to the first 10 amino acids (1–10) of the N terminus of histone H3 inhibited interaction of LKR with histone H3, whereas a peptide corresponding to the C terminus (amino acids 74–83) had no significant effect (Fig. 4 B). A peptide consisting of amino acids 10–20 also showed some competition for histone H3 (Fig. 4 B). This suggests that dLKR/SDH interacts with the N-terminal region of H3.

RNAi and overexpression data suggest that dLKR/SDH acts as a negative regulator of ecdysone-induced transcription. This is supported by the fact that histone H3 methylation by CARMER, a positive regulator of transcription, is specifically inhibited by dLKR/SDH. Therefore, we assessed the effect of the coexpression of
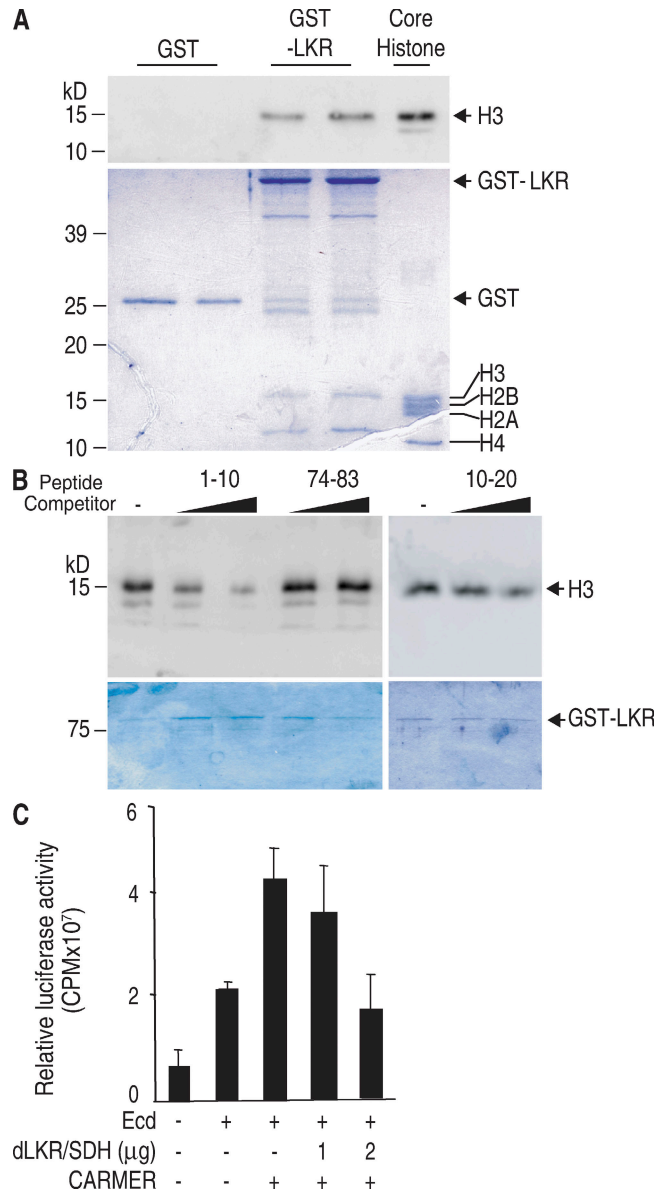

Figure 4. **dLKR/SDH interacts directly with the N-terminal region of H3 and H4 and represses CARMER-mediated transcription.** (A) 2 μg of recombinant GST or GST-LKR was incubated with calf thymus histones and pulled down using glutathione Sepharose beads, and half of the pull-down was separated by SDS-PAGE and blotted with histone H3 antibody. The other half was stained with Coomassie Brilliant blue (bottom), showing both histone H3/H4, GST, and GST-LKR. The second and fourth lanes do not contain NADH and α-ketoglutarate, and the fifth lane is calf thymus bulk histones alone to show the migration of H3, H2B, H2A, and H4. GST and GST LKR is shown. (B) 10 μg of histones was incubated with 2 μg of GST-LKR in the presence of increasing amounts of histone peptide competitors corresponding to histone H3 amino acids 1–10, 10–20, and 74–83. Pull-downs were performed and blotted for histone H3. One half of the pull-down was stained with Coomassie Brilliant blue showing GST-LKR. (C) Transfections and luciferase assays were performed as in Fig. 2 using 1 μg pEcR-Luc reporter and 0.4 μg pIE-CARMER. Where indicated, ethanol (−) or ecdysone (Ecd +) was used. Error bars represent SD.

dLKR/SDH and CARMER in a reporter assay (Fig. 4 C). Ecdysone treatment induced activity of the ecdysone-responsive reporter, and this was further enhanced by coexpressing CARMER (Fig. 4 C). When CARMER and dLKR/SDH were coexpressed, dLKR/SDH inhibited CARMER-mediated transcription (Fig. 4 C).
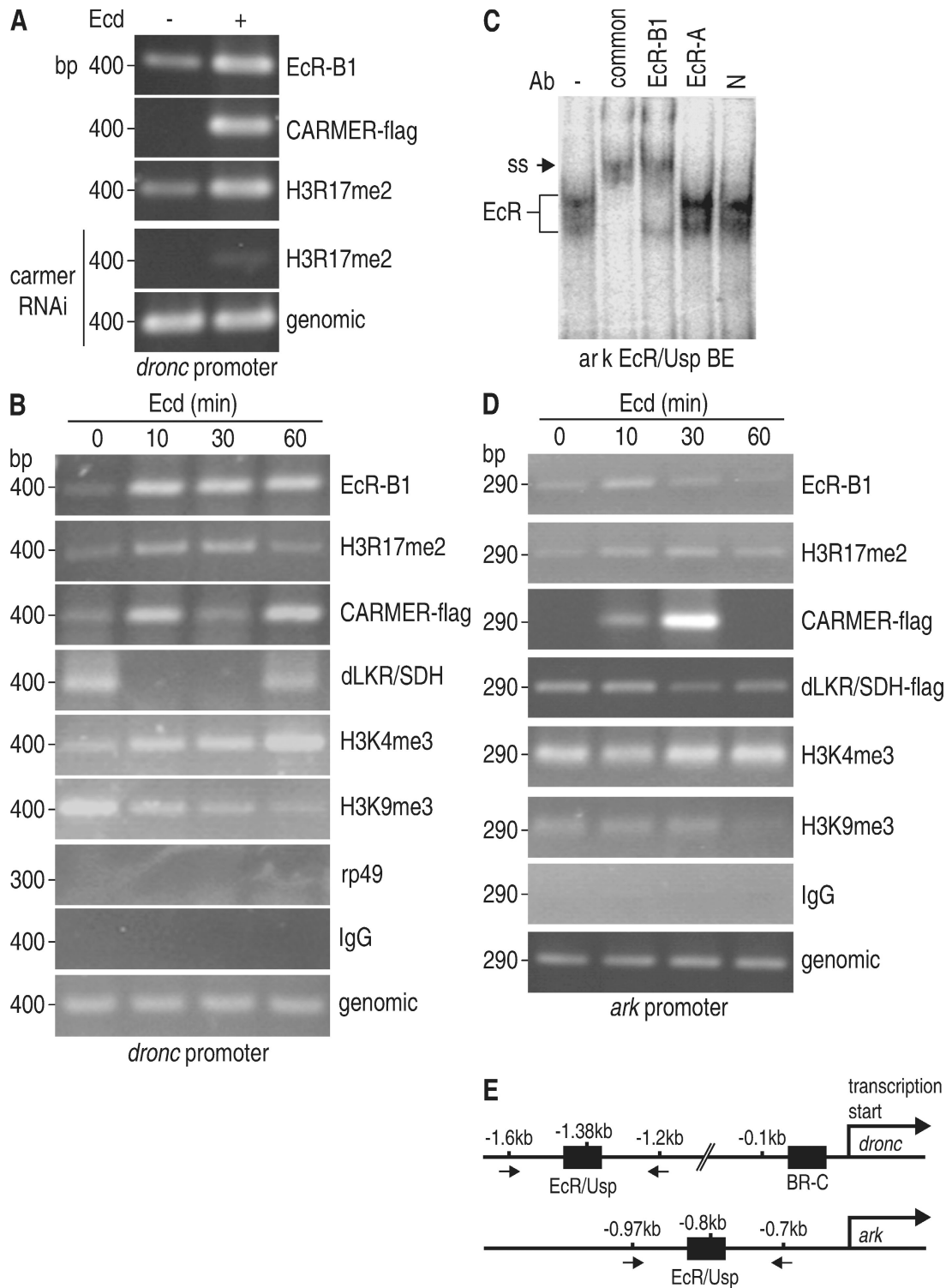
Figure 5.   **dLKR/SDH is recruited to the endogenous *dronc* and *ark* promoters.** (A) For ChIP analyses, 10^7 *l*(2)mbn cells were treated with ethanol (−) or ecdysone (+) for 30 min, and cross-linked chromatin was immunoprecipitated with EcR-B1 antibody, flag antibody for CARMER, and histone H3R17me2–specific antibody. CARMER was also knocked down by RNAi, and H3R17me2 was assessed. Input control represents 20% of genomic DNA from each treatment taken before the immunoprecipitation. For the detection of flag-CARMER, cells were transfected as outlined in Materials and methods with pIE CARMER. (B) Cells were treated as in A, but ecdysone treatment was performed for 10, 30, and 60 min. The indicated methylation-specific antibodies, dLKR/SDH antibody, and Ig control antibody (preimmune serum) were used for ChIP. *rp49* was amplified as a control for the dLKR/SDH immunoprecipitation. Input DNA is shown (genomic). (C) EMSA was performed by ^{32}P labeling an oligonucleotide spanning the potential EcR/Usp BE of the *ark* promoter and incubating with 9 μg of nuclear extract and 1 μg EcR antibody that recognizes all isoforms (common), B1 isoform, α isoform, and control antibody N27A1 (N). Complexes were resolved on a 5% Tris/borate/EDTA acrylamide gel, dried, and exposed to a screen. ss, antibody super shift. (D) Genomic DNA samples from the same immunoprecipitations used in B were used to amplify regions of the *ark* promoter spanning the EcR/Usp BE. For the detection of flag-CARMER and dLKR/SDH, 2×10^7 cells were transfected for each time point. (E) Schematic diagrams of *dronc* and *ark* promoters showing the locations of primers (arrows) used for ChIP analyses.

dLKR/SDH is recruited to hormone-responsive promoters, regulating the kinetics of H3 arginine methylation

ChIP assays were performed to determine the mechanism of action for dLKR/SDH. In the absence of ecdysone, there was very little EcR-B1 or CARMER recruited to the *dronc* promoter, correlating with low levels of H3R17me2 (Fig. 5 A). After ecdysone treatment, there was an increase in EcR-B1 recruitment on the promoter, coinciding with the recruitment of CARMER and correlating with the appearance of H3R17me2 (Fig. 5 A). *Carmer* knockdown by RNAi led to a significant decrease in ecdysone-induced H3R17me2, suggesting that CARMER is responsible for H3R17me2 (Fig. 5 A). Detailed analysis of the kinetics of histone methylation showed recruitment of EcR-B1 to the promoter as early as 10 min after ecdysone treatment, which remained stable until 1 h (Fig. 5 B). H3R17me2 methylation appeared after 10 min of ecdysone treatment and was present at 30 min; however, by 1 h it had diminished, suggesting the dynamic nature of this modification (Fig. 5 B). As expected, CARMER was recruited by 10 min, coinciding with the appearance of H3R17me2; however, it had disengaged by 30 min and surprisingly reappeared by 1 h, when H3R17me2 was less abundant. A very low level of H3K4me3 was detected in the absence of ecdysone, but it rapidly increased by 10 min after ecdysone treatment. The levels of H3K4me3 increased with time up to 1 h, which is consistent with its role as a positive regulator of transcription. A high level of H3K9me3 was detected in untreated cells; however, in response to ecdysone treatment, H3K9me3 rapidly decreased with time consistent with its role as a repressor of transcription (Fig. 5 B). Recruitment of endogenous dLKR/SDH to the promoter was also assessed using the specific antibody. dLKR/SDH was present on the promoter in untreated cells but disappeared by 10 min of ecdysone treatment and reappeared at 1 h (Fig. 5 B), with its appearance inversely correlating with the appearance of H3R17me2.

We also examined the recruitment of these coactivators to the endogenous *ark* promoter. By electrophoretic mobility shift assay (EMSA), we found an EcR/Usp BE that lies 807 bp upstream of the transcription start site (Fig. 5 E). This site specifically binds the EcR-B1 isoform but not the A isoform (Fig. 5 C). ChIP analysis showed that a low level of EcR-B1 was associated with the *ark* promoter, which increased by 10 min of ecdysone treatment followed by a decrease at 30 and 60 min (Fig. 5 D). This is in contrast to the kinetics of recruitment to the *dronc* promoter. H3R17me2 methylation was also evident by 10 and 30 min of ecdysone treatment. However, by 1 h it had diminished. Flag-tagged dLKR/SDH was present on the promoter in untreated cells and cells treated with ecdysone for 10 min; however, a decrease was evident at 30 min and 1 h (Fig. 5 D). Recruitment of CARMER was evident by 10 min, reaching a maximum at 30 min, followed by a decrease by 60 min. H3K4me3 increased from 30 min onwards, and H3K9me3 decreased in response to ecdysone treatment with time. Collectively, these results demonstrate that by 10 min after ecdysone treatment, increased recruitment of EcR-B1 coincides with the recruitment of CARMER and the presence of H3R17me2.

After 30 min of ecdysone treatment, this is followed by a rapid decline. Although CARMER is recruited again at 1 h (for *dronc* promoter), this does not coincide with H3R17me2 at that time, as dLKR/SDH presumably inhibits H3R17me2.

Common to both *dronc* and *ark* promoters, the presence of endogenous dLKR/SDH seems inversely proportional to H3R17me2, which is present mostly at the time when H3R17me2 does not occur or at the beginning of its appearance. It is also present at 1 h, as is CARMER, although H3R17me2 does not occur at this time. Based on these data, we conclude that dLKR/SDH inhibits H3R17me2 methylation when present on the promoter. This was confirmed by knocking down dLKR/SDH by RNAi and assessing changes in arginine methylation along the *dronc* promoter. Cells treated with control dsRNA showed the appearance of H3R17me2 by 7 min after ecdysone treatment, reaching maximum levels at 30 min and a decrease at 1 h (Fig. 6 A). Knockdown of dLKR/SDH resulted in a dramatic shift in the kinetics of H3R17me2 methylation, with levels at a maximum between 4–7 min and decreased again from 10 min onwards (Fig. 6 A). This experiment was validated by semiquantitative real-time PCR of the ChIP-enriched DNA and was compared with total input genomic DNA (Fig. 6 B). The results clearly show that H3R17me2 is generally low along the *dronc* promoter, with levels increasing at 10–30 min of ecdysone treatment and decreasing by 1 h. When dLKR/SDH was knocked down, in the absence of ecdysone, there is no significant difference in the levels of H3R17me2. However, as early as 4 min of hormone treatment, H3R17me2 levels increase sharply and then steadily decrease. These results indicate that dLKR/SDH inhibits H3R17me2 when occupying the promoter and controls kinetics of methylation at the promoter.

Global levels of H3R17me2 are elevated in dLKR/SDH RNAi-treated *Drosophila* cells

We next wanted to assess whether global levels of H3R17me2 were affected after dLKR/SDH knockdown. Given that the histone code states that individual histone modifications may affect the methylation status at other residues (Groth et al., 2007; Kouzarides, 2007), we also examined other histone methylation marks. Knockdown of dLKR/SDH showed a clear increase of H3R17me2 (Fig. 7). In contrast, the levels of H3K4me3 or H3K27me2 remained largely unchanged (Fig. 7).

dLKR/SDH fine-tunes the developmental expression of hormone-induced genes in *Drosophila*

dLKR/SDH expression was found to be dynamic throughout development, with transcript levels low in early embryos (0–8 h) and first instar larvae (L1) and highest at the time of larval/pupal metamorphosis (white prepupae; Fig. 8 A). In the salivary glands, the low levels of expression at 2 h before head eversion (Fig. 8 B, −2 hRHE) increased dramatically at head eversion (0 h) and decreased 2 h later (Fig. 8 B).

To study the in vivo function of dLKR/SDH in ecdysone-mediated transcription, we generated transgenic flies to knock-down or overexpress dLKR/SDH specifically in salivary glands. The larval salivary glands have been used as an experimental
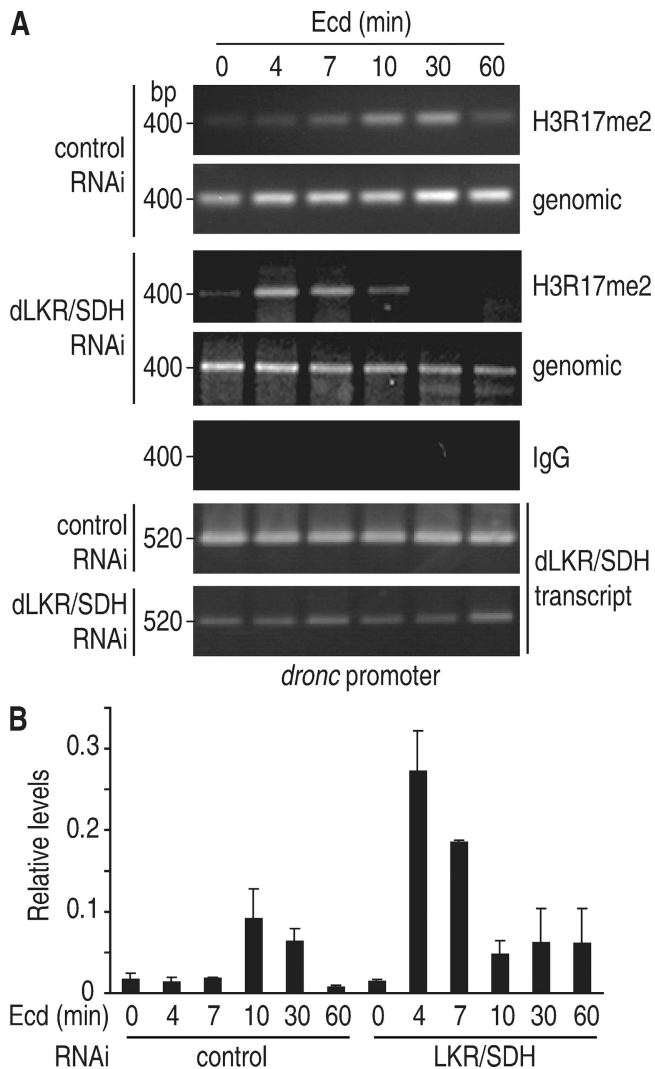
A

dronc promoter

B

Figure 6. **dLKR/SDH regulates the dynamics of histone H3R17me2.** (A) 10^7 *l*(2)mbn cells were treated with either double-stranded RNA to control (Ndfip2) or dLKR/SDH for 48 h. Cells were then treated with ethanol (0) or ecdysone. ChIP assays were performed as outlined in Fig. 5. RNA was purified from the first extraction step and converted to cDNA, and the levels of dLKR/SDH transcript were detected by RT-PCR (dLKR/SDH transcript). (B) Antibody-enriched genomic DNA used in A and input genomic DNA per treatment were used in semiquantitative real-time PCR. Relative levels were determined by comparing the levels of DNA from the immunoprecipitated samples to the corresponding input genomic DNA. Error bars represent SEM.

model to assess ecdysone-mediated transcription. Overexpression and knockdown of dLKR/SDH were confirmed by immunoblotting and real-time PCR, and the levels of *dronc* transcript were analyzed by real-time PCR (Fig. 8, C–E). In wild-type salivary glands, *dronc* transcript increased after the ecdysone pulse at the time of head eversion (0–1 h after head eversion; Fig. 8 E). Consistent with the results in *l*(2)mbn cells (Fig. 3 A), knockdown of dLKR/SDH in salivary glands resulted in an increase in *dronc* transcript 1 h before and 1 h after head eversion (Fig. 8 E), whereas overexpression of dLKR/SDH had no significant effect on the expression levels. Therefore, we conclude that dLKR/SDH mediates the correct timing of the developmental induction of ecdysone-regulated genes.
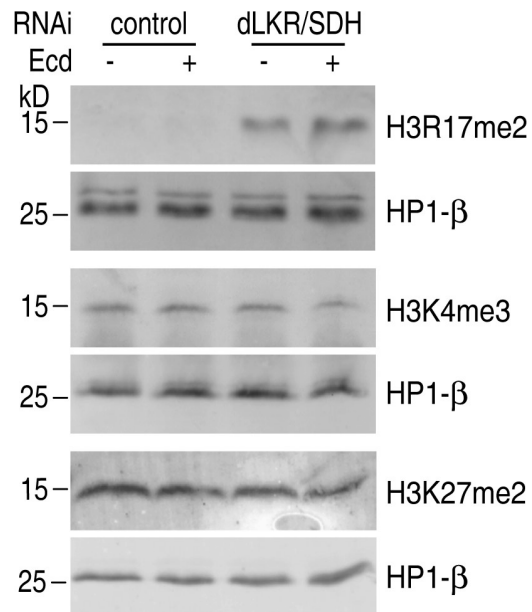

Figure 7. **Knockdown of dLKR/SDH results in global up-regulation of H3R17me2.** *Drosophila l*(2)mbn cells were treated with double-stranded RNA to Ndfip2 (control) or dLKR/SDH (dLKR/SDH) and treated with either ethanol (−) or ecdysone (+) for 4 h. Lysates were prepared, and 75 μg was separated by SDS-PAGE, transferred to a membrane, and blotted with histone H3 methyl–specific antibodies as shown. The same membranes were blotted with HP1-β antibody as a loading control. For the detection of H3R17me2, 100 μg of protein was loaded onto the gel.

dLKR/SDH is required for normal development

To further study the in vivo function of dLKR/SDH, we examined a gene deficiency that disrupts the *dLKR/SDH* locus. The homozygous deficiency (*Df/Df*) produced viable adult flies that exhibit significantly smaller (P < 0.0001) wing size (Fig. 8, F and G) and reduced overall body weight (not depicted). To confirm the role of dLKR/SDH in *Drosophila* development, we examined the effect of knocking down dLKR/SDH during wing development using the *en-GAL4* driver. As in the *Df/Df* flies, the adult RNAi lines showed significantly smaller (P < 0.001) wings when compared with control flies (Fig. 8, F and G), confirming that the phenotype is caused by a specific loss of dLKR/SDH.

dLKR/SDH genetically interacts with EcR/Usp

To study the endogenous dLKR/SDH and EcR interaction, we tested whether reducing dLKR/SDH by RNAi modified the phenotype of overexpression of a dominant-negative EcR allele (*EcR^{F645A}*) in the *Drosophila* eye using the *GMR-GAL4* driver. As previously reported (Sedkov et al., 2003), specific overexpression of *EcR^{F645A}* in the eye disrupts differentiation of the ommatidia and eye patterning. This results in a decrease in pigment cells, collapse of the eye, and characteristic scarring (Fig. 8 H). Knockdown of dLKR/SDH partially restored the pigmentation defect and displayed a striking decrease of scarring. Therefore, reducing dLKR/SDH by RNAi resulted in suppression of the *EcR^{F645A}* rough eye phenotype. We also analyzed the genetic interaction between *dLKR/SDH* and *EcR* in the wing.
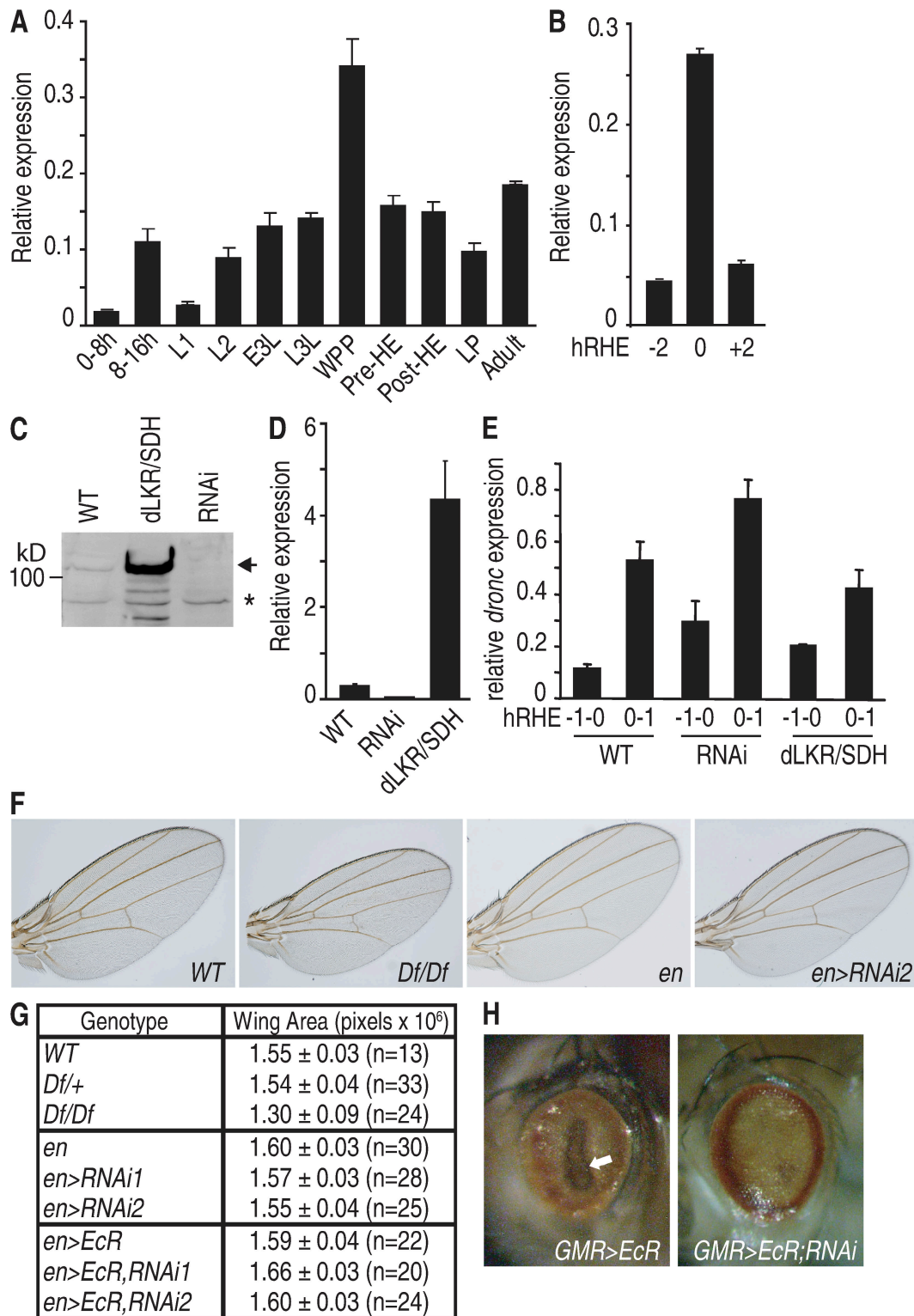
Figure 8. **dLKR/SDH is dynamically expressed during development, genetically interacts with EcR/Usp to control the timing of transcription, and influences wing development.** (A) Expression of *dLKR/SDH* during development. Real-time PCR was performed in duplicate, and the mRNA expression levels were normalized against the internal control gene *rp49*. The error bars represent SEM. WPP, white prepupae. (B) Expression of *dLKR/SDH* during salivary gland programmed cell death. Real-time PCR was performed as in A using salivary gland cDNA at the indicated stages of development. −2, 0, and +2 refer to hours after head eversion (hRHE), corresponding to the endogenous ecdysone pulse. (C) 20 µg of salivary gland lysates from animals at 0 h after head eversion were analyzed by immunoblotting using the dLKR/SDH antibody. Salivary glands from wild type (WT) and those expressing salivary gland (sgs3-GAL4)–specific dLKR/SDH transgenic (dLKR/SDH) or dLKR/SDH double-stranded RNA (RNAi) were used. dLKR/SDH bands are indicated by an arrow. The asterisk indicates a nonspecific protein of ∼65 kD detected by the dLKR/SDH antibody. (D) Real-time PCR was performed as in A using salivary gland cDNA from animals as in C. (E) Effects of dLKR/SDH on *dronc* expression in salivary glands. Real-time PCR was performed as in A. The developmental stages are indicated as hours after head eversion. (F) Wing size was decreased in homozygous (*Df/Df*) adult females compared with wild-type controls. Knockdown of dLKR/SDH in the posterior wing compartment using en-GAL4 (en>RNAi2) resulted in a smaller wing compared with the control, en-GAL4 (en).

Inhibition of EcR function by the expression of EcR^{F645A} had no effect on wing size; however, EcR^{F645A} expression restored the small wing phenotype caused by a knockdown of dLKR/SDH (Fig. 8 G). These results support the interaction of dLKR/SDH with EcR and the role of dLKR/SDH as a negative regulator of ecdysone-mediated transcription.

Discussion

We have identified a novel cofactor involved in ecdysone-mediated regulation of gene expression. Surprisingly, this cofactor is an enzyme involved in lysine catabolism (Sacksteder et al., 2000). The fact that this gene is transcriptionally up-regulated in larval salivary glands undergoing programmed cell death in response to rising levels of ecdysone as well as in response to γ irradiation (Lee et al., 2003) prompted us to further characterize it. We established that dLKR/SDH binds directly to EcR/Usp in vitro, and this interaction occurs both in the absence and presence of ecdysone. This differed from the template assay, in which dLKR/SDH was recruited only in the presence of hormone. We believe that the complexes formed on oligonucleotides in this system are unstable, and therefore we could only detect dLKR/SDH and other factors in the presence of hormone, which is believed to increase the affinity of cofactors for their receptors.

With the use of reporter assays and RNAi in cells and in *Drosophila*, we found that dLKR/SDH is a repressor of ecdysone-induced transcription of *dronc* and *ark*. Its repressive effect is consistent with the fact that dLKR/SDH inhibits ecdysone-inducible H3R17me2. The greatest effect of dLKR/SDH knockdown on transcription was evident at 6 h of ecdysone treatment. This is likely the result of the active transcription of these genes occurring in the first 12 h of ecdysone treatment in *l(2)mbn* cells. Any effects on active transcription will therefore be more evident at earlier time points (i.e., 6 h) rather than later time points (i.e., 24 h). *ark* transcription is also more affected at 6 h than *dronc*, which may reflect different modes of *ark* and *dronc* regulation by ecdysone. For example, although *ark* seems primarily regulated by direct EcR/Usp binding, *dronc* is known to be additionally regulated by other ecdysone-inducible transcription factors such as BR-C and E93 (for review see Kumar and Cakouros, 2004).

Our experiments show that dLKR/SDH does not demethylate histones but potently inhibits arginine methylation of histone H3 by CARMER. Although we could not detect any interaction with CARMER, dLKR/SDH specifically interacted with H3 and H4 via its LKR domain but not H2B and H2A. This is intriguing given that arginine methylation occurs preferentially on H3 and H4 (Bedford and Richard, 2005). The absence of any modifications by full-length dLKR/SDH on histone H3 allows us to speculate that ketoglutarate might be important for

dLKR/SDH to adopt a conformation required to sterically inhibit CARMER for methylating histone H3. This scenario is somewhat similar to the mechanism used by the corepressor C-terminal binding protein, which represses transcription using NADH (Zhang et al., 2002), and Sir2, which uses NAD^+ (Imai et al., 2000). Given that dLKR/SDH and its homologues recognize lysine, it was surprising that it did not affect methylation of lysine on histone H3. In fact, we have mutated H3K4 and H3K9, and these mutations do not affect the interaction between dLKR/SDH and histone H3 (unpublished data). Therefore, it is highly likely that a group of amino acids within the N terminus are important for the interaction of dLKR/SDH with histone H3 and that the conformation adopted by dLKR/SDH specifically inhibits H3R17me2. We are currently examining the mechanisms involved in more detail.

Endogenous dLKR/SDH is present in the cytosol, consistent with its possible role in lysine catabolism, and in the nucleus, where its levels seem to fluctuate in a time-dependent manner in response to hormone treatment. Apart from histones, protein arginine methyltransferases are involved in methylating several other substrates (Bedford and Richard, 2005). In fact, the predominant arginine methyltransferase in human cells, PRMT1, is responsible for 85% of all arginine methylations and for methylating H4R3 when recruited by nuclear receptors (Pawlak et al., 2000; Tang et al., 2000). In addition, it has also been shown to methylate heterogenous nuclear RNP, which is involved in pre-mRNA processing and transport (Liu and Dreyfuss, 1995). PRMT1 lacks a nuclear localization signal, is localized preferentially in the cytoplasm, and shuttles into the nucleus by associating with other proteins entering the nucleus. Only when methylation is inhibited can PRMT1 be seen to accumulate in the nucleus (Herrmann et al., 2005). It is predicted that PRMT1 is attached to unmethylated substrates such as newly synthesized heterogenous nuclear RNP molecules (Herrmann et al., 2005). It is thus possible that dLKR/SDH is regulated in a similar manner, as it has no nuclear localization signal but does have a putative nuclear export signal. It is also possible that dLKR/SDH might regulate methylation in other cellular compartments. Given its ability to inhibit H3R17me2, it is not surprising that mechanisms exist to prevent its accumulation in the nucleus, where it could prevent H3R17me2 for prolonged periods of time and hinder the hormonal response. Although dLKR/SDH can bind EcR/Usp, our ChIP data show that dLKR/SDH is on the promoter spanning the BE before EcR/Usp is recruited. It is therefore more feasible that another constitutive factor is responsible for recruiting dLKR/SDH and interacting with histone H3, and its cycling back onto the promoter at 1 h of ecdysone treatment might be mediated by its ability to interact with EcR/Usp.

The ChIP data after dLKR/SDH knockdown demonstrated the premature appearance of H3R17me2 as well as the premature

---

(G) Wing areas as measured using the histogram tool in Photoshop. *Df/Df* adult females had a significantly smaller wing area than wild-type and *Df/+* control animals (P < 0.0001). dLKR/SDH RNAi lines 1 and 2 expressed using en-GAL4 also resulted in a significantly smaller wing (P = 0.0006 and P < 0.0001 for RNAi line 1 and line 2, respectively). Interaction with the EcR^{F645A} dominant-negative allele alleviated this decrease in size. Significance was calculated using a *t* test. (H) Genetic interaction tests using GMR-GAL4–driven expression of dLKR/SDH RNAi and EcR^{F645A} (GMR>EcR;RNAi) in the eye resulted in suppression of the characteristic scar (arrow) caused by EcR^{F645A} expression (GMR>EcR).
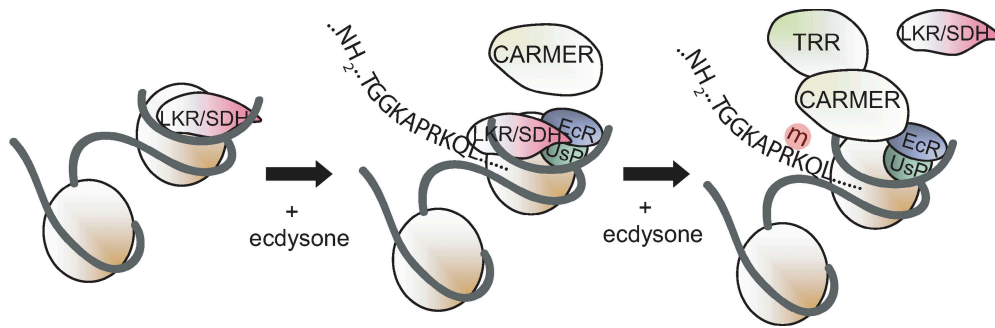
Figure 9. **A model for dLKR/SDH function.** In this model, dLKR/SDH is present on the EcR/Usp BE via its interaction with EcR/Usp. In the presence of ecdysone, CARMER is recruited to the promoter, but dLKR/SDH inhibits its ability to methylate histone H3 on R17 as a result of its ability to bind H3 and hinder methylation. Eventually, dLKR/SDH is removed, and methylation proceeds. The methyl mark is then removed, dLKR/SDH is recruited followed by CARMER, and the cycle is repeated.

loss of H3R17me2, confirming that the role of dLKR/SDH is to control the kinetics of H3R17me2. Based on our in vitro data, this occurs by inhibiting methylation by the positive regulator CARMER. It has been documented that H3R17me2 serves to recruit RNA polymerase II to the promoter, and removal of H3 arginine methylation is needed for elongation of RNA polymerase II (Metivier et al., 2003). Therefore, this may explain why the change in H3R17me2 kinetics by dLKR/SDH knockdown results in a dramatic shift in transcription kinetics, as the initiation and elongation of the RNA polymerase could possibly occur more frequently when dLKR/SDH is knocked down. The only other enzyme capable of inhibiting R17 methylation is PADI4 in mammals, which is also involved in amino acid catabolism (Cuthbert et al., 2004). However, a PADI4 homologue is not present in *Drosophila*, which prompts us to conclude that dLKR/SDH may be functionally equivalent in flies.

Knockdown of dLKR/SDH in the salivary glands resulted in a premature increase in the expression of *dronc* but, in spite of this, showed no discernible alterations in tissue histolysis or metamorphosis. Furthermore, dLKR/SDH-deficient flies or ones harboring tissue-specific RNAi do not show strong phenotypes. Given that dLKR/SDH is a negative regulator of ecdysone-induced gene expression, these phenotypes suggest that dLKR/SDH plays a fine-tuning role as opposed to an essential role for ecdysone-regulated transcription. The mild phenotypes observed for alterations in dLKR/SDH are not surprising given the phenotypes observed for some other histone-modifying enzymes such as the histone demethylases LSD1 and Lid. *Drosophila LSD1* homozygous mutants are viable but sterile despite showing alterations in the pattern of histone methylation (Rudolph et al., 2007), and overexpression of *lid* during eye differentiation had no effect on the adult phenotype (Secombe et al., 2007). Nevertheless, dLKR/SDH can genetically interact with the ecdysone receptor in the eye and wing, and loss of dLKR/SDH results in specific developmental phenotypes in the wing. The smaller wing size (in both deficiency and RNAi lines) is suggestive of defects in the regulation of cell growth, proliferation, and/or differentiation. We measured wing hair density in dLKR/SDH knockdown compared with control and observed no change, indicating that cell size is not altered (unpublished data). We are currently investigating alternative pathways that

are mediated by dLKR/SDH and whether these effects are involved in the phenotypes observed in vivo.

Our current work supports a model shown in Fig. 9 in which dLKR/SDH binds the promoter region spanning the EcR/Usp BE. In response to hormone, there is an increase in EcR/Usp binding to the *dronc* and *ark* promoters followed by recruitment of CARMER within 10 min. However, the LKR domain of dLKR/SDH already bound to histone H3 shields H3R17 from methylation. dLKR/SDH is then removed by an unknown mechanism from the promoter, allowing CARMER to methylate H3R17. Between 30 and 45 min of hormonal stimuli, H3R17me2 is removed, followed by the recruitment of dLKR/SDH and CARMER by 1 h. dLKR/SDH therefore serves to control the correct developmental timing of ecdysone-induced genes such as *dronc* and *ark* in *Drosophila* at least partly by controlling histone H3R17 methylation kinetics.

Materials and methods

Cell culture and antibodies
*l(2)*mbn cells (a gift from A. Dorn, Johannes Gutenburg University, Mainz, Germany) were cultured as previously described (Cakouros et al., 2002). Ecdysone (Sigma-Aldrich) was used at 10 μM. Transfected SF21 insect cells were grown in SFII 900 complete medium and blasticidin at 20 μg/ml for selection. Antibodies to DRONC and DRICE have been described previously (Dorstyn et al., 2002). Antibodies to EcR-B1 (AD4.4), EcR-A (15G1a), EcR common (DDA2.7), HP1-β (C1A9), and armadillo (N27A1) were purchased from Developmental Studies Hybridoma Bank (University of Iowa). Histone H3 antibody was obtained from Cell Signaling Technology, H3R17me2 antibody was purchased from Abcam, and all other methylation-specific antibodies were obtained from Millipore.

Generation of constructs
CG7144 (dLKR/SDH) cDNA was prepared from 5 μg *Drosophila* embryo RNA using the Superscript II kit (Invitrogen). Full-length flag-tagged dLKR/SDH was cloned into the *Drosophila* pIE1-4 expression vector using restriction site SacII or pIB/V5-His with SacII for insect cell expression and purification. The dLKR/SDH mutant construct carrying Gly to Ala substitutions in residues 221, 223, and 228 was cloned into pIB/V5-His vector. These amino acids are conserved within the NADH-binding domain of various homologues. pIE CARMER expression vectors have been previously described (Cakouros et al., 2004a). EcoRI-containing primers were used to clone full-length dLKR/SDH into pUAST for tissue-specific expression in *Drosophila*. For tissue-specific RNAi, a hairpin was cloned into pUAST. pEcR-Luc consists of the EcR/Usp BE of the heat shock 27 promoter cloned in front of the luciferase reporter described previously (Cakouros et al., 2004a). BR-C Luc consists of the proximal promoter of *dronc*, which contains multiple BR-C BEs cloned in front of the luciferase reporter described

previously (Cakouros et al., 2002). For expressing dsRNA in *l*(2)mbn cells, the region of dLKR/SDH amino acids 657–834 was cloned into pGEMT-easy and used for in vitro transcription using T7/Sp6. Control dsRNAi construct containing mammalian Ndfip2 cDNA has been previously described (Cakouros et al., 2002). For expression of recombinant LKR (amino acids 1–457) and SDH domains (amino acids 420–928) as GST fusion proteins, they were cloned into pGEX2TK. To generate a polyclonal antibody for dLKR/SDH, the region encoding amino acids 779–926 was cloned into pGEX2TK, and purified protein was used to immunize rabbits. Antibodies were purified by first depletion of the GST antibodies through a GST-agarose column followed by affinity purification on a dLKR/SDH (amino acids 779–926)-agarose column.

RNA extractions, Northern blotting, and PCR
RNA extraction and Northern blotting was performed as previously described (Cakouros et al., 2002). An *ark* probe was generated by PCR using forward (5′-GGTGGCGTCGGCACACAGTGCC-3′) and reverse primers (5′-GCGGTGTCAAGGCGTCAGGG-3′). The RT-PCR and primers used were described previously (Cakouros et al., 2004b).

Semiquantitative real-time PCR
Total RNA was isolated from *Drosophila* salivary glands using TRIZOL reagent (Invitrogen). cDNA was synthesized using Superscript II Reverse transcription (Invitrogen) and oligo dT (Geneworks) from 5 μg of total RNA. Real-Time PCR was performed on a thermal cycler (Rotor-Gene 3000; Corbett Research) using RT^2 Real-Time SYBR green/ROX PCR MasterMix (Superarray) according to the manufacturer's instructions. The following primer sets were used: *dLKR/SDH* forward (5′-CGAGAACCTCAAGCAGAAGC-3′) and reverse (5′-ATTGATTCCACGCTCCTCAC-3′), *dronc* forward (5′-CAGCATC-GTAGGCTCCTATTG-3′) and reverse (5′-ATATGGCACTATCCCCACCA-3′), and *rp49* forward (5′-GCCACCAGTCGGATCGATATGCTA-3′) and reverse (5′-GGTTCTATTGAGAACGCAGGCGACCGTT-3′). Reactions were performed in triplicate, and the mRNA expression levels were normalized against the internal control gene *rp49* using the $\Delta\Delta C_T$ method.

Transfection and luciferase assays
1 μg pEcR Luc reporter or pBR-C Luc was transfected using Cellfectin (Invitrogen) together with 100 ng EcR-B1 expression construct and different levels of pIB-dLKR/SDH. 400 ng pIE-CARMER was cotransfected where indicated with pIE-dLKR/SDH, pEcR-Luc, or pBR-C Luc. Where indicated, 2 μg pIE–BR-C expression construct was also used together with pIE-dLKR/SDH. Each transfection contained equal amounts of DNA using the pIE1-4 or pIB expression vector and was performed as described previously (Cakouros et al., 2002). All transfections were performed in parallel with pxpG empty reporter vector and values subtracted from those of the promoter-reporter construct.

EMSA
Nuclear extracts and EMSA were performed as previously described (Cakouros et al., 2002, 2004b). The sequence of the probes used was 5′-CACACAAACATAACAAGTTCATTCACAGGGCAAACTCAGTGACG-3′.

Oligonucleotides and primers
Primers used for cloning dLKR/SDH into pIE were forward (5′-GACCCGC-GGATGTGGCGAGTGATTCAACTGCGCGC-3′) and reverse (5′-GACCCG-CGGTTACTTGTCATCGTCGTCATTTAGCCATCTGGAGGTTTCC-3′) containing flag tag sequence. Primers used for cloning dLKR/SDH into pIB/V5-His were forward (5′-ACCGAACCGCGGTGGCGAGTGATTCAACTGCGCG-3′) containing a SacII site and reverse (5′-ACCGAACCGCGGATTTAGCCAT-CTGGAGGTTTC-3′) containing a SacII site. The primer used to mutate amino acids 221, 223, and 228 to Ala was 5′-CTTACATTTGTGTTCACT-GCCTCTGCAAATGTTTCCCAAGCTGCCCAGGAGGTG-3′. For cloning dLKR/SDH into pUAST, forward primer (5′-CAGGAATTCGAGATGTGGC-GAGTGATTCAACTGCGC-3′) containing an EcoRI site and reverse primer (5′-CAGGAATTCTTACTTGTCATCGTCGTCATTTAGCCATCTGGAGGTTT-CCG-3′) containing an EcoRI site and flag tag sequence were used. For the construction of tissue-specific RNAi for dLKR/SDH, the following primers were used: RNAi 1A (5′-CAGGAATTCATGGAGGGAAGTTCGGAGTCT-GAC-3′) containing an EcoRI site, RNAi 1B (5′-CAGGGTACCCTGGCGC-CACGTGACATCCGG-3′) containing a Kpn1 site, RNAi 2A (5′-CAGCTC-GAGATCGAGGGAAGTTCGGAGTCTGAC-3′) containing an Xho1 site, and RNAi 2B (5′-CAGGGTACCGGAATCCCTGTTGGGGAAACC-3′) containing a Kpn1 site. To clone a portion of dLKR/SDH into pGEM for use in in vitro transcription, forward (5′-GGTCACCCAGGGGAGTACTTCT-3′) and reverse (5′-CCCGCTCGAAGGCAAGTCTCTT-3′) primers were used. Primers

used for GST-dLKR/SDH were LKR forward (5′-CGCGAATTCCGTGGC-GAGTGATTCAACTGCGCGCA-3′) and reverse (5′-CGCGAATTCTTACTT-GTCATCGTCGTCGCCCTCCGTCAGCTGACCGTTGCT-3′ and 5′-CGC-GAATTCTTACTTGTCATCGTCGTCATTTAGCCATCTGGAGGTTTCCGT-3′). For immobilized template bead assay, the primers used were wild type (5′-CAAAGGCCAAAGACCCACAACTTTTTC-3′). Oligonucleotides containing specific EcR/Usp BE mutations were also biotinylated at the 5′ end. The mutant primer was 5′-CAAAAACTAAAGACCCACAACTTTTTC-3′. *dronc* ChIP primer sequences used were forward (5′-CTATGCAATGCTAATTG-GCAGCCCC-3′) and reverse (5′-AGGAATTTAGCACACAGAGC-3′). *ark* primers used were forward (5′-GCGTGCAGGTGAAAGCTTATGTACC-3′) and reverse (5′-GAGGAGGCGAGCAGTTACAGCATCT-3′). For *rp49*, forward (5′-GCCACCAGTCGGATCGATATGCTA-3′) and reverse (5′-GGTTC-TATTGAGAACGCAGGCGACCGTT-3′) primers were used.

Immobilized template bead assay
1.5 × 10^8 *l*(2)mbn cells were treated with 10 μM ecdysone for 2 h, and nuclear extracts were prepared as previously described (Cakouros et al., 2002). Extracts were precleared with 100 μl streptavidin Sepharose beads (GE Healthcare) and 50 μg of salmon sperm DNA. Double-stranded oligonucleotides spanning the *dronc* promoter from region −1,308 to −1,281 bp relative to the transcription start site were biotinylated at the 5′ end of the sense strand. 500 μl streptavidin Sepharose beads were washed three times in buffer T (10 mM Tris, pH 7, 1 mM EDTA, 1 M NaCl, and 0.1% NP-40) and blocked for 1 h in 3.6 ml of buffer T supplemented with 50 mg/ml BSA. To 1 ml of slurry, 50 μg of double-stranded annealed oligonucleotide was added and incubated on a rotating wheel for 2 h at 4°C. Streptavidin bead–oligonucleotide complexes were then washed three times with buffer Z (25 mM Hepes, pH 7.8, 12.5 mM MgCl$_2$, 20% glycerol, and 0.1% NP-40). Five pull-downs were set up per treatment (with or without ecdysone), each with 100 μl of bead/oligonucleotide, 100 μg of nuclear extract, 800 μl of buffer Z, 50 μg of salmon sperm DNA, 100 mM NaCl, 20 μg poly(dIdC), and complete protease inhibitors. After overnight incubation at 4°C, complexes were washed twice in buffer Z supplemented with 100 mM NaCl, and beads were boiled in 2× SDS loading buffer and separated on a 10% SDS-PAGE. The gel was stained with Coomassie Brilliant blue, and appropriate bands were excised and identified by mass spectrometry at the Adelaide Proteomics Centre.

Liquid chromatography–tandem mass spectrometry and protein identification
The excised bands were washed three times in 50 μl of ammonium bicarbonate (100 mM) containing 50% acetonitrile (HPLC grade; Merck) and again in 100% acetonitrile. 25 μl trypsin (500 ng of modified porcine trypsin, 2 mM acetic acid, 80 mM ammonium bicarbonate, and 8% acetonitrile [vol/vol]) was then added to rehydrate the spots. Proteolytic digestion was allowed to occur at 37°C for 16 h. Tryptic peptides were reduced by the addition of 1 μl of 0.1 M tris-(carboxyethyl)phosphine, and the tryptic digestion was stopped by the addition of 25 μl formic acid (1% vol/vol). The supernatant was collected, and the protein was further extracted in 25 μl acetonitrile (100%). The combined extracts were reduced in volume to ~10 μl in a Speed-Vac system (Savant Instruments, Inc.) before liquid chromatography–mass spectrometry/mass spectrometry analysis. Peptides were introduced into a mass spectrometer (Micromass Q-Tof2; Waters) through a NanoSpray source coupled to a CapLC system (Waters). Injected samples were desalted on a C18 precolumn (0.3 × 3 mm, 5-μm packing; LC-Packings) before separation on an analytical column (0.075 × 50 mm, 3-μm packing; Atlantis dC18; Waters) using an acetonitrile gradient (5–70% containing 0.1% formic acid) at a flow rate of 200 nl/min.

Eluted peptides were ionized through the NanoSpray source with 3 kV. A 7-s survey scan of the eluting material identified multiple charged species (2, 3, and 4 charge states), and the most abundant (<4) were selected for fragmentation and mass spectrometry/mass spectrometry analysis. After signal had been accumulated for each of the fragment ion series for up to 21 s, the system reverted to the survey scan mode to identify further multiply charged species of potential interest. After acquisition, mass spectrometry/mass spectrometry data were processed and analyzed using ProteinLynx 2.0 software (Waters). De novo sequence tags were determined from the fragmentation data and used to search the National Centre for Biotechnology Information nonredundant protein database for protein identification matches. Matched proteins were assessed for quality and validity of the identification. In all cases, at least two separate peptide sequences were used to assign a match.

In vitro methylation inhibition assay

Recombinant dLKR and SDH were expressed as GST-tagged proteins in BL21 star LysS *Escherichia coli*, and thrombin was cleaved to remove the GST tag. In a 25-µl reaction, 4 µg of calf thymus histones was incubated with 100–500 ng of recombinant LKR or SDH in buffer (100 mM KH$_2$PO$_4$, 1 mM EDTA, pH 6.8, 200 µM NADH, and 2 mM α-ketoglutarate). Where indicated, both NADH and α-ketoglutarate were omitted. After incubation at 30°C for 4 h, 30 µl histone methylation buffer (Cakouros et al., 2004b) was then added with 5 µl S-adenosyl [^{3}H]Met and 1 µg GST-CARMER or TRR (provided by A. Mazo, Kimmel Cancer Center, Philadelphia, PA). Histone methylation was performed by incubation at 30°C for 90 min followed by SDS-PAGE in duplicate gels. One gel was Coomassie stained, whereas the other was fixed (25% isopropanol and 10% glacial acetic acid) for 20 min, incubated with Amplify (GE Healthcare) for 30 min, dried down, and exposed to hyperfilm for 5 d.

Production of full-length dLKR/SDH

His-tagged full-length dLKR/SDH was cloned into pIB/V5His. The expression construct was transfected into SF21 cells, and stable transfectants were generated by maintaining cells with blasticidin at 20 µg/ml. For protein purification, 10^8 cells were washed in PBS and resuspended in 20 ml of lysis buffer (50 mM Tris, pH 7.8, 150 mM NaCl, 1% NP-40, and complete protease inhibitors). Cells were lysed by freeze thawing, and cleared supernatant was incubated with 400 µl Ni^{2+}–nitrilotriacetic acid agarose beads overnight at 4°C. Beads were washed in lysis buffer three times and protein eluted with 1 M imidazole. Purified protein was dialysed overnight in 100 mM NaCl/20 mM Tris-HCl, pH 7.6 (plus complete protease inhibitors).

dLKR/SDH enzyme assays

5 µg of purified protein was incubated with 1 mM NADH, 2 mM α-ketoglutarate, and 14 mM lysine in a total volume of 50 µl (made up with 100 mM phosphate buffer, pH 6.8) in 96-well plates. Reaction was performed at room temperature for up to 4 h. Background levels not attributed to NADH were measured using buffer without NADH and values subtracted from the measurements with enzyme and NADH. Measurements were made at excitation and emission wavelengths of 340 nm and 455 nm, respectively, with an emission slit width of 2 nm using a luminescence spectrometer (LS55; PerkinElmer).

ChIP

1–2 × 10^7 *l*(2)mbn cells were cultured in 6-well dishes with or without 10 µM ecdysone. ChIP assay was performed as described previously (Shi et al., 2004). DNA was purified on spin columns (Ultraclean; MO BIO) and resuspended in 50 µl Tris/EDTA. 3 µl of purified DNA was used for PCR with annealing at 55°C and extension for 1.5 min. To detect EcR-B1 and flag-tagged CARMER or flag-dLKR/SDH recruitment, 37 cycles were used, whereas 33 cycles were used to detect H3R17me2, H3K4me3, and H3K9me3. 39 cycles were used for the Ig control, dLKR/SDH, and genomic input control.

Fly stocks, maintenance, and analyses

Df(2L)ED496 fly stock that removes dLKR/SDH and a least one other gene was obtained from the Szeged *Drosophila* Stock Center. UAS-EcR^{F645A}, GMR-GAL4, sgs3-GAL4, and en-GAL4 stocks were obtained from the Bloomington *Drosophila* Stock Center. Wing analysis was performed using flies grown at 25°C by dehydrating adult flies in xylene and mounting wings in Canada Balsam. Samples were photographed using a microscope with a 4× UPlan Fl objective (BX51; Olympus) and a camera (DP70; Olympus) at room temperature. Images were captured with Olysia Bioreport software (Olympus) and compiled using Photoshop version 6.0 (Adobe). The wing areas were measured using the magnetic lasso tool and histogram function in Photoshop. Tissue-specific expression in the eye was driven using GMR-GAL4 and genetic interaction tests with UAS-EcR^{F645A} performed at 18°C because of the severe lethality of the UAS-EcR^{F645A} allele at 25°C. Eye images were acquired using a camera (DP11; Olympus) attached to a stereozoom microscope (SZ40; Olympus) with a 2× auxiliary objective at room temperature. Images were processed using Photoshop.

Online supplemental material

Fig. S1 shows localization of dLKR/SDH in transfected cells. Fig. S2 shows quantification of the RNAi-mediated knockdown of dLKR/SDH. Online supplemental material is available at http://www.jcb.org/cgi/content/full/jcb.200712169/DC1.

References

Akdemir, F., R. Farkas, P. Chen, G. Juhasz, L. Medved'ova, M. Sass, L. Wang, X. Wang, S. Chittaranjan, S.M. Gorski, et al. 2006. Autophagy occurs upstream or parallel to the apoptosome during histolytic cell death. *Development.* 133:1457–1465.

Ballas, N., E. Battaglioli, F. Atouf, M.E. Andres, J. Chenoweth, M.E. Anderson, C. Burger, M. Moniwa, J.R. Davie, W.J. Bowers, et al. 2001. Regulation of neuronal traits by a novel transcriptional complex. *Neuron.* 31:353–365.

Bannister, A.J., R. Schneider, and T. Kouzarides. 2002. Histone methylation: dynamic or static? *Cell.* 109:801–806.

Bedford, M.T., and S. Richard. 2005. Arginine methylation an emerging regulator of protein function. *Mol. Cell.* 18:263–272.

Bhattacharjee, J.K. 1985. α-Amino-adipate pathway for the biosynthesis of lysine in lower eukaryotes. *Crit. Rev. Microbiol.* 12:131–151.

Cakouros, D., T. Daish, D. Martin, E.H. Baehrecke, and S. Kumar. 2002. Ecdysone-induced expression of the caspase DRONC during hormone-dependent programmed cell death in *Drosophila* is regulated by Broad-Complex. *J. Cell Biol.* 157:985–995.

Cakouros, D., T.J. Daish, and S. Kumar. 2004a. Ecdysone receptor directly binds the promoter of the *Drosophila* caspase dronc, regulating its expression in specific tissues. *J. Cell Biol.* 165:631–640.

Cakouros, D., T.J. Daish, K. Mills, and S. Kumar. 2004b. An arginine-histone methyltransferase, CARMER, coordinates ecdysone-mediated apoptosis in *Drosophila* cells. *J. Biol. Chem.* 279:18467–18471.

Chen, D., H. Ma, H. Hong, S.S. Koh, S.M. Huang, B.T. Schurter, D.W. Aswad, and M.R. Stallcup. 1999. Regulation of transcription by a protein methyltransferase. *Science.* 284:2174–2177.

Cuthbert, G.L., S. Daujat, A.W. Snowden, H. Erdjument-Bromage, T. Hagiwara, M. Yamada, R. Schneider, P.D. Gregory, P. Tempst, A.J. Bannister, and T. Kouzarides. 2004. Histone deimination antagonizes arginine methylation. *Cell.* 118:545–553.

Daish, T.J., D. Cakouros, and S. Kumar. 2003. Distinct promoter regions regulate spatial and temporal expression of the *Drosophila* caspase dronc. *Cell Death Differ.* 10:1348–1356.

Daish, T.J., K. Mills, and S. Kumar. 2004. *Drosophila* caspase DRONC is required for specific developmental cell death pathways and stress-induced apoptosis. *Dev. Cell.* 7:909–915.

Dorstyn, L., P.A. Colussi, L.M. Quinn, H. Richardson, and S. Kumar. 1999. DRONC, an ecdysone-inducible *Drosophila* caspase. *Proc. Natl. Acad. Sci. USA.* 96:4307–4312.

Dorstyn, L., S.H. Read, D. Cakouros, J.R. Huh, B.A. Hay, and S. Kumar. 2002. The role of cytochrome *c* in caspase activation in *Drosophila melanogaster* cells. *J. Cell Biol.* 156:1089–1098.

Goncalves-Butruille, M., P. Szajner, E. Torigoi, A. Leitte, and P. Arruda. 1996. Purification and characterisation of the bifunctional enzyme lysine-ketoglutarate reductase-saccharopine dehydrogenase from maize. *Plant Physiol.* 110:765–771.

Groth, A., W. Rocha, A. Verreault, and G. Almouzni. 2007. Chromatin challenges during DNA replication and repair. *Cell.* 128:721–733.

Herrmann, F., J. Lee, M.T. Bedford, and F.O. Fackelmayer. 2005. Dynamics of human protein arginine methyltransferase 1 (PRMT1) in vivo. *J. Biol. Chem.* 280:38005–38010.

Imai, S., C.M. Armstrong, M. Kaeberlein, and L. Guarente. 2000. Transcriptional silencing and longevity protein Sir2 is an NAD-dependent histone deacetylase. *Nature.* 403:795–800.

Klose, R.J., E.M. Kallin, and Y. Zhang. 2006. JmjC-domain-containing proteins and histone demethylation. *Nat. Rev. Genet.* 7:715–727.

Kouzarides, T. 2007. Chromatin modifications and their function. *Cell.* 128:693–705.

Kumar, S., and D. Cakouros. 2004. Transcriptional control of the core cell-death machinery. *Trends Biochem. Sci.* 29:193–199.

Lee, C.Y., C.R. Simon, C.T. Woodard, and E.H. Baehrecke. 2002. Genetic mechanism for the stage- and tissue-specific regulation of steroid triggered programmed cell death in *Drosophila*. *Dev. Biol.* 252:138–148.

Lee, C.Y., E.A. Clough, P. Yellon, T.M. Teslovich, D.A. Stephan, and E.H. Baehrecke. 2003. Genome-wide analyses of steroid- and radiation-triggered programmed cell death in *Drosophila*. *Curr. Biol.* 13:350–357.

Li, B., M. Carey, and J.L. Workman. 2007. The role of chromatin during transcription. *Cell.* 128:707–719.

Liu, Q., and G. Dreyfuss. 1995. In vivo and in vitro arginine methylation of RNA-binding proteins. *Mol. Cell. Biol.* 15:2800–2808.

Metivier, R., G. Penot, M.R. Hubner, G. Reid, H. Brand, M. Kos, and F. Gannon. 2003. Estrogen receptor-alpha directs ordered, cyclical, and combinatorial recruitment of cofactors on a natural target promoter. *Cell.* 115:751–763.

Mills, K., T. Daish, K.F. Harvey, C.M. Pfleger, I.K. Hariharan, and S. Kumar. 2006. The *Drosophila melanogaster* Apaf-1 homologue ARK is required for most, but not all, programmed cell death. *J. Cell Biol.* 172:809–815.

Pawlak, M.R., C.A. Scherer, J. Chen, M.J. Roshon, and H.E. Ruley. 2000. Arginine N-methyltransferase 1 is required for early postimplantation mouse development, but cells deficient in the enzyme are viable. *Mol. Cell. Biol.* 20:4859–4869.

Rudolph, T., M. Yonezawa, S. Lein, K. Heidrich, S. Kubicek, C. Schafer, S. Phalke, M. Walther, A. Schmidt, T. Jenuwein, and G. Reuter. 2007. Heterochromatin formation in *Drosophila* is initiated through active removal of H3K4 methylation by the LSD1 homolog SU(VAR)3-3. *Mol. Cell.* 26:103–115.

Sacksteder, K.A., B.J. Biery, J.C. Morrell, B.K. Goodman, B.V. Geisbrecht, R.P. Cox, S.J. Gould, and M.T. Geraghty. 2000. Identification of the α-aminoadipic semialdehyde synthase gene, which is defective in familial hyperlysinemia. *Am. J. Hum. Genet.* 66:1736–1743.

Schurter, B.T., S.S. Koh, D. Chen, G.J. Bunick, J.M. Harp, B.L. Hanson, A. Henschen-Edman, D.R. Mackay, M.R. Stallcup, and D.W. Aswad. 2001. Methylation of histone H3 by coactivator-associated arginine methyltransferase 1. *Biochemistry.* 40:5747–5756.

Secombe, J., L. Li, L. Carlos, and R.N. Eisenman. 2007. The Trithorax group protein Lid is a trimethyl histone H3K4 demethylase required for dMyc-induced cell growth. *Genes Dev.* 21:537–551.

Sedkov, Y., E. Cho, S. Petruk, L. Cherbas, S.T. Smith, R.S. Jones, P. Cherbas, E. Canaani, J.B. Jaynes, and A. Mazo. 2003. Methylation at lysine 4 of histone H3 in ecdysone-dependent development of *Drosophila*. *Nature.* 426:78–83.

Shi, Y., and J. Whetsine. 2007. Dynamic regulation of histone lysine methylation by demethylases. *Mol. Cell.* 25:1–14.

Shi, Y., F. Lan, C. Matson, P. Mulligan, J.R. Whetstine, P.A. Cole, R.A. Casero, and Y. Shi. 2004. Histone demethylation mediated by the nuclear amine oxidase homolog LSD1. *Cell.* 119:941–953.

Strahl, B.D., and C.D. Allis. 2000. The language of covalent histone modifications. *Nature.* 403:41–45.

Tang, J., A. Frankel, R.J. Cook, S. Kim, W.K. Paik, K.R. Williams, S. Clarke, and H.R. Herschman. 2000. PRMT1 is the predominant type I protein arginine methyltransferase in mammalian cells. *J. Biol. Chem.* 275:7723–7730.

Tsai, C.C., and J.D. Fondell. 2004. Nuclear receptor recruitment of histone-modifying enzymes to target gene promoters. *Vitam. Horm.* 68:93–122.

Truman, J.W., and L.M. Riddiford. 2002. Endocrine insights into the evolution of metamorphosis in insects. *Annu. Rev. Entomol.* 47:467–500.

Tsukada, Y., J. Fang, H. Erdjument-Bromage, M.E. Warren, C.H. Borchers, P. Tempst, and Y. Zhang. 2006. Histone demethylation by a family of JmjC domain-containing proteins. *Nature.* 439:811–816.

Wang, H., Z.Q. Huang, Q. Feng, H. Erdjument-Bromage, B.D. Strahl, S.D. Briggs, C.D. Allis, J. Wong, P. Tempst, and Y. Zhang. 2001. Methylation of histone H4 at arginine 3 facilitating transcriptional activation by nuclear hormone receptor. *Science.* 293:853–857.

Yin, V.P., and C.S. Thummel. 2005. Mechanisms of steroid-triggered programmed cell death in *Drosophila*. *Semin. Cell Dev. Biol.* 16:237–243.

Zhu, X., G. Tang, and G. Galili. 2000. The catabolic function of the α-aminoadipic acid pathway in plants is associated with unidirectional activity of lysine-oxoglutarate reductase, but not saccharopine dehydrogenase. *Biochem. J.* 351:215–220.

Zhang, Q., D.W. Piston, and R.H. Goodman. 2002. Regulation of corepressor function by nuclear NADH. *Science.* 295:1895–1897.